Research on the Multibeam Bathymetry Problem in Uneven Seabeds Based on Computational Geometry

Mingkai Li*, Haokun He#, Jiyang Liu#

School of Mathematics and Statistics, Shandong University, Weihai, Shandong, 264209, China

* Corresponding Author Email: 202100820072@mail.sdu.edu.cn

#These authors contributed equally.

Abstract. The principle of the multibeam seabed bathymetry system involves emitting dozens to hundreds of beams at once in a plane perpendicular to the course, and then receiving the acoustic waves returned by the seabed through the receiving transducer. This paper will study through computational geometry how to calculate information such as seabed depth, survey line coverage width, and the overlap rate between survey lines based on the received information in uneven seabed areas. This study first discusses the special case where the survey line is parallel to the contour line, defining coverage width and overlap rate. It then uses the sine theorem and triangle solving to calculate physical quantities such as seawater depth, coverage width, and overlap rate with the previous survey line when the seabed has a slope. Sensitivity analysis is conducted from three aspects: depth, slope, and opening angle. This research continues to discuss the general case where the survey line is not parallel to the contour line. By first calculating the angle between the intersection line generated by the seabed section detected by the vessel and the seabed slope surface and the horizontal plane, the problem is transformed into the model under the parallel situation to continue the calculation and solve the coverage width. The study of multibeam bathymetry in uneven seabeds using computational geometry enables the application of multibeam bathymetry in uneven seabed areas, providing a simple calculation method for the field of bathymetry in uneven seabeds and expanding the application conditions of multibeam bathymetry.

Keywords: Multibeam bathymetry, Computational Geometry, Sensitivity Analysis.

1. Introduction

1.1. Background of the Problem

In the technology of water depth measurement, common methods include single-beam bathymetry and multibeam bathymetry, both of which use the principle of sound wave propagation to measure the depth of water. Single-beam bathymetry, due to its point-by-point continuous measurement, results in dense bathymetric data along the track but lacks data between different survey lines. It only involves a single beam contacting the seafloor, presenting certain disadvantages. The multibeam bathymetry system is an evolution based on single-beam bathymetry. It can emit multiple beams simultaneously and receive acoustic signals reflected back from the seafloor. The advantage of this system is that it can measure a full-coverage depth strip with a certain width in areas where the seafloor is flat, thereby improving the efficiency and accuracy of water depth measurement.

A key issue in using multibeam bathymetry systems is how to determine the appropriate survey line spacing to meet overlap requirements. The overlap rate is the proportion of coverage overlap between adjacent survey lines, affecting the quality and efficiency of the measurement. If the interval between survey lines is too large, there will be data omission; if too small, data redundancy occurs. In practical applications, the undulating changes in seabed topography are often significant, making the determination of appropriate survey line spacing even more complex. Using average water depth to design survey line intervals might lead to data omission in shallower areas, while using the shallowest depth could result in excessive data overlap in deeper areas, affecting data processing and measurement efficiency. Therefore, how to determine an appropriate survey line arrangement in multibeam bathymetry systems to meet the requirements of data integrity and quality under different seabed topographical conditions while maintaining measurement efficiency is an important technical

challenge. The development of this technology is of significant importance for exploring seabed geomorphological conditions.

1.2. Literature Review

The development history of multibeam seabed bathymetric technology can be traced back to the mid-20th century. Initially, this technology was mainly used for naval applications, such as submarine navigation and underwater intelligence gathering. Over time, multibeam seabed bathymetry technology gradually entered the civilian domain, including oceanography, geology, marine resource exploration, and marine engineering [1].

Research methods in multibeam seabed bathymetry include: multibeam data acquisition and processing technology for obtaining high-resolution seabed topographical data; acoustic propagation modeling and sound speed profile modeling to improve bathymetry accuracy; analysis of backscatter data to identify and classify seabed objects; and data fusion techniques to integrate multibeam data with other sensor data for comprehensive marine surveying.

Significant progress has been made in the field of multibeam seabed bathymetry, but challenges remain. Researchers are continuously improving data processing algorithms to enhance the accuracy of depth measurement and expand the scope of technological applications. Moreover, with the increasing demand for deep-sea exploration, multibeam seabed bathymetry technology is also evolving to accommodate more complex seabed environments and task requirements.

1.3. Research Objectives

This study embarks from the necessity to explore more complex seabed environments, deliberating on the application of multibeam bathymetric systems in uneven seabed areas. It focuses on utilizing received acoustic information in these irregular seabed regions to compute variables such as seabed depth, the coverage width of survey lines, and the overlap rate between these lines.

In the specific scenario where the survey lines are parallel to the isobaths, and there is an angle formed by the intersection line of the plane perpendicular to the survey line direction and the seabed slope, and the vessel's survey line runs parallel to the seabed slope, we aim to establish a model. This model will solve for the seawater depth, coverage width, and the overlap rate with the preceding survey line at various distances from a central point. For a more intuitive demonstration, this research has constructed a simulated seabed landscape for practical calculations. This simulation sets the scenario with the multibeam transducer's opening angle at 120°, a slope of 1.5°, and a specific case of the seawater depth at the sea area's central point being 70 meters. It calculates the seawater depth, coverage width, and overlap rate with the previous survey line at different distances from the center point [2].

In the general situation where the survey lines are not parallel to the isobaths, and there is an angle present between the direction of the survey line and the normal direction of the seabed slope, we plan to develop a model. This model will decipher the coverage width of survey lines that are at varying distances from a central point and concurrently maintain a certain angle with the seabed slope. For ease of visual representation, this research has also established a simulated seabed terrain for actual computations. This terrain sets up the scenario with the multibeam transducer's opening angle at 120°, a slope of 1.5°, and a specific case of the seawater depth at the sea area's central point being 120 meters, calculating the coverage width of each survey line [3].

2. Research Methods

2.1. Problem Analysis for the Special Case of Survey Lines Parallel to Isobaths

In this study, considering real-world circumstances and known background conditions such as the transducer's opening angle, the seabed slope, and the seawater depth at the sea area's central point, the problem can be transformed into a planar geometric triangle-solving issue once the distance of

the survey line from the center point is determined. By employing mathematical methods like the Law of Sines and angle conversions, the task of solving the triangle can be successfully accomplished.

2.2. Problem Analysis for the General Case of Survey Lines Not Parallel to Isobaths

Similar to the special case where survey lines are parallel to isobaths, with the same known conditions such as the transducer's opening angle, the seabed slope, and the central seawater depth, once we determine the angle of the survey line direction and the distance of the vessel from the center, we can ascertain the vessel's sea surface position. This allows us to transform the problem into a three-dimensional geometric issue. In this 3D geometric context, the fundamental problem we need to solve is to find the angle between the detection coverage line and the horizontal plane. Consequently, we can convert this general non-parallel model into the special case model of survey lines parallel to isobaths [4].

3. Results and Analysis

3.1. Results and Analysis in the Special Case of Survey Lines Parallel to Isobaths

3.1.1 Model Establishment and Solution in the Special Case of Survey Lines Parallel to Isobaths

In this study, a planar geometric model can be directly established for the coverage width of multibeam bathymetry and between adjacent strips[5]. As shown in Figure 1, we set E, O as the positions of the ship's survey line and the central position, respectively. Simultaneously, for ease of geometric analysis, this study abstracts related geographical positions into point surfaces and marks them with uppercase letters.

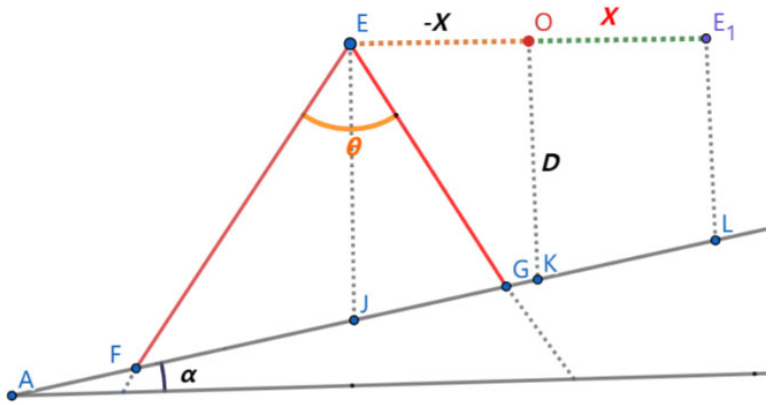

Figure 1. Determining the Depth at the Location of the Survey Line

Step 1: Determine the seabed depth at the survey line position

As shown in Figure 1, When examining the coverage width of a certain survey line, the first step is to determine the seabed depth at the location of the survey line to facilitate subsequent calculations. For this study, we can initially use the single-beam bathymetric system to measure the depth at one point in the center of the sea area. Then, suppose there is a survey line passing through the center O and the seabed depth at that point is D, which is used as a reference for calculating the seabed depth of the remaining survey lines.

In this study, we assume that another survey line is at a distance X from the central survey line at O.When the ship is to the right of the center point O, X is positive.When the ship is to the left of the center point O, $X$is negative. Therefore, the seabed depth at the corresponding survey line position can be represented as:

$$|EJ| = D - Xtan(\alpha) \tag{1}$$

Step 2: Determine the Coverage Width at the Survey Line Position

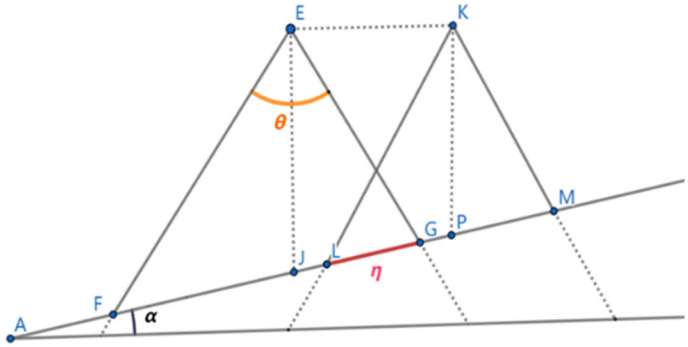

Figure 2. Determining the Coverage Width at the Location of the Survey Line

As shown in Figure 2, α,θ.the depth at the ship's position $|EJ|$ and the distance between survey lines $|EK|$. First, we can determine the angles $\angle EFG$ and $\angle EGF$ based on the principles that the sum of the internal angles of a triangle is π (180 degrees) and that vertically opposite angles are equal:

$$\angle EFG = \frac{\pi - \theta}{2} - \alpha \tag{2}$$

$$\angle EGF = \pi - \angle EFG - \theta \tag{3}$$

$$\Rightarrow \angle EGF = \frac{\pi - \theta}{2} + \alpha \tag{4}$$

Next, consider two adjacent survey lines, E and K. Focusing on the coverage width of survey line E, and starting from the practical implication of coverage width, as shown in Figure 2, survey line E can detect the full depth within the range of $|FG|$. Therefore, this study defines coverage width as the length of the seafloor slope that can be measured within the opening angle θ. It can be verified by substitution that the definition of coverage width given in the problem statement for a flat seabed with parallel survey lines is a special case under our definition.

Consequently, from the above figure, we know the coverage width $W = |FG|$. In $\triangle EFG$, we know that:

$$|FG| = |JG| + |FJ| \tag{5}$$

In triangles $\triangle EJG$ and $\triangle EJF$, we utilize the Law of Sines to derive:

$$\begin{cases} \dfrac{|JG|}{sin(\angle JEG)} = \dfrac{|JG|}{sin\left(\frac{\theta}{2}\right)} = \dfrac{|EJ|}{sin(\angle EGF)} = \dfrac{|EJ|}{cos\left(\alpha - \frac{\theta}{2}\right)} \\ \dfrac{|FJ|}{sin(\angle FEJ)} = \dfrac{|FJ|}{sin\left(\frac{\theta}{2}\right)} = \dfrac{|EJ|}{sin(\angle EFG)} = \dfrac{|EJ|}{cos\left(\alpha + \frac{\theta}{2}\right)} \end{cases} \tag{6}$$

$$\Rightarrow \begin{cases} |JG| = \dfrac{|EJ|sin\left(\frac{\theta}{2}\right)}{cos\left(\alpha - \frac{\theta}{2}\right)} \\ |FJ| = \dfrac{|EJ|sin\left(\frac{\theta}{2}\right)}{cos\left(\alpha + \frac{\theta}{2}\right)} \end{cases} \tag{7}$$

$$\Rightarrow W = |FG| = \frac{|EJ|sin\left(\frac{\theta}{2}\right)}{cos\left(\alpha - \frac{\theta}{2}\right)} + \frac{|EJ|sin\left(\frac{\theta}{2}\right)}{cos\left(\alpha + \frac{\theta}{2}\right)} \tag{8}$$

Step 3: Calculating the Overlap Rate between the Survey Line and the Previous Line

In the setup of this study, the seabed is not flat, and the coverage widths of two survey lines are not equal[6]. To calculate the overlap rate with the previous line, for example, for two lines E and K as shown in Figure 2, we adopt the following definition for the overlap rate: the length of the repeated measurements on a section perpendicular to the survey lines divided by the coverage width of the previous line on that section. That is:

$$\eta = \frac{|LG|}{|FG|} = \frac{|JG| + |LP| - |JP|}{|FG|} \tag{9}$$

$$|EK| = d \tag{10}$$

This can be validated by substitution, confirming that the overlap rate definition $\eta = 1 - \frac{d}{W}$ for a flat seabed with parallel survey lines is a special case in our context.

Applying the Law of Sines in $\triangle EJG$:

$$\frac{|LP|}{sin(\angle LKP)} = \frac{|LP|}{sin\left(\frac{\theta}{2}\right)} = \frac{|KP|}{sin(\angle KLM)} = \frac{|KP|}{cos\left(\alpha + \frac{\theta}{2}\right)} \tag{11}$$

From which we derive:

$$|LP| = \frac{|KP| sin\left(\frac{\theta}{2}\right)}{cos\left(\alpha + \frac{\theta}{2}\right)} \tag{12}$$

Considering side JP, by employing the properties of a right trapezoid, we can establish:

$$|JP| = \frac{|EK|}{cos(\alpha)} \tag{13}$$

Similarly, we have:

$$|KP| = |EJ| - |EK| tan(\alpha) \tag{14}$$

Summarizing the above, we arrive at:

$$\eta = \frac{|LG|}{|FG|} = \frac{|JG| + |LP| - |JP|}{|FG|} \tag{15}$$

$$\Rightarrow \eta = \frac{\frac{|EJ| sin\left(\frac{\theta}{2}\right)}{cos\left(\alpha - \frac{\theta}{2}\right)} + \frac{|KP| sin\left(\frac{\theta}{2}\right)}{cos\left(\alpha + \frac{\theta}{2}\right)} - \frac{|EK|}{cos(\alpha)}}{\frac{|EJ| sin\left(\frac{\theta}{2}\right)}{cos\left(\alpha - \frac{\theta}{2}\right)} + \frac{|EJ| sin\left(\frac{\theta}{2}\right)}{cos\left(\alpha + \frac{\theta}{2}\right)}} \tag{16}$$

$$\Rightarrow \eta = \frac{\frac{|EJ| sin\left(\frac{\theta}{2}\right)}{cos\left(\alpha - \frac{\theta}{2}\right)} + \frac{\left(|EJ| - |EK| tan(\alpha)\right) sin\left(\frac{\theta}{2}\right)}{cos\left(\alpha + \frac{\theta}{2}\right)} - \frac{|EK|}{cos(\alpha)}}{\frac{|EJ| sin\left(\frac{\theta}{2}\right)}{cos\left(\alpha - \frac{\theta}{2}\right)} + \frac{|EJ| sin\left(\frac{\theta}{2}\right)}{cos\left(\alpha + \frac{\theta}{2}\right)}} \tag{17}$$

$$\Rightarrow \eta = \frac{\frac{[D - Xtan(\alpha)]sin\left(\frac{\theta}{2}\right)}{cos\left(\alpha - \frac{\theta}{2}\right)} + \frac{[D - Xtan(\alpha) - dtan(\alpha)]sin\left(\frac{\theta}{2}\right)}{cos\left(\alpha + \frac{\theta}{2}\right)} - \frac{d}{cos(\alpha)}}{[D - Xtan(\alpha)]\left\{\frac{sin\left(\frac{\theta}{2}\right)}{cos\left(\alpha - \frac{\theta}{2}\right)} + \frac{sin\left(\frac{\theta}{2}\right)}{cos\left(\alpha + \frac{\theta}{2}\right)}\right\}} \quad (18)$$

3.1.2 Computational Results Simulating Seabed Topography

For a more intuitive demonstration, this study established a simulated seabed topography for practical calculations. This specific scenario set up involves a multibeam transducer with a beam angle of 120°, a slope of 1.5°, and a water depth of 70 m at the central point of the sea area[7]. The results for this scenario are calculated as follows.

Table 1. Computational Results of Simulated Seabed Topography

Distance from the center point/m	Water depth/m	Coverage width/m	Overlap rate with the previous survey line/%
-800	90.949	315.813	——
-600	85.712	297.628	33.640
-400	80.474	279.442	30.949
-200	75.237	261.256	25.712
0	70	243.07	19.782
200	64.763	224.884	13.781
400	59.526	206.699	6.808
600	54.288	188.513	-1.391
800	49.051	170.327	-11.172

Given the known parallelism of the survey lines with the slope, and considering the slope is deeper in the west and shallower in the east, the results are analyzed as follows:

(1) With equidistant survey lines, the water depth forms an arithmetic sequence, with a depth difference of approximately $5.237m$ every 200 meters.

(2) Under the same equidistant condition, the coverage width also follows an arithmetic sequence, with a difference of approximately $18.185m$ every 200 meters.

(3) For the overlap rate with the previous survey line under equidistant conditions, it does not form an arithmetic sequence, and although the overlap rate increases with increasing depth, the rate of increase slows down.

As shown in Figure 3: The chart illustrates the impact of the distance from the center point on various parameters.:

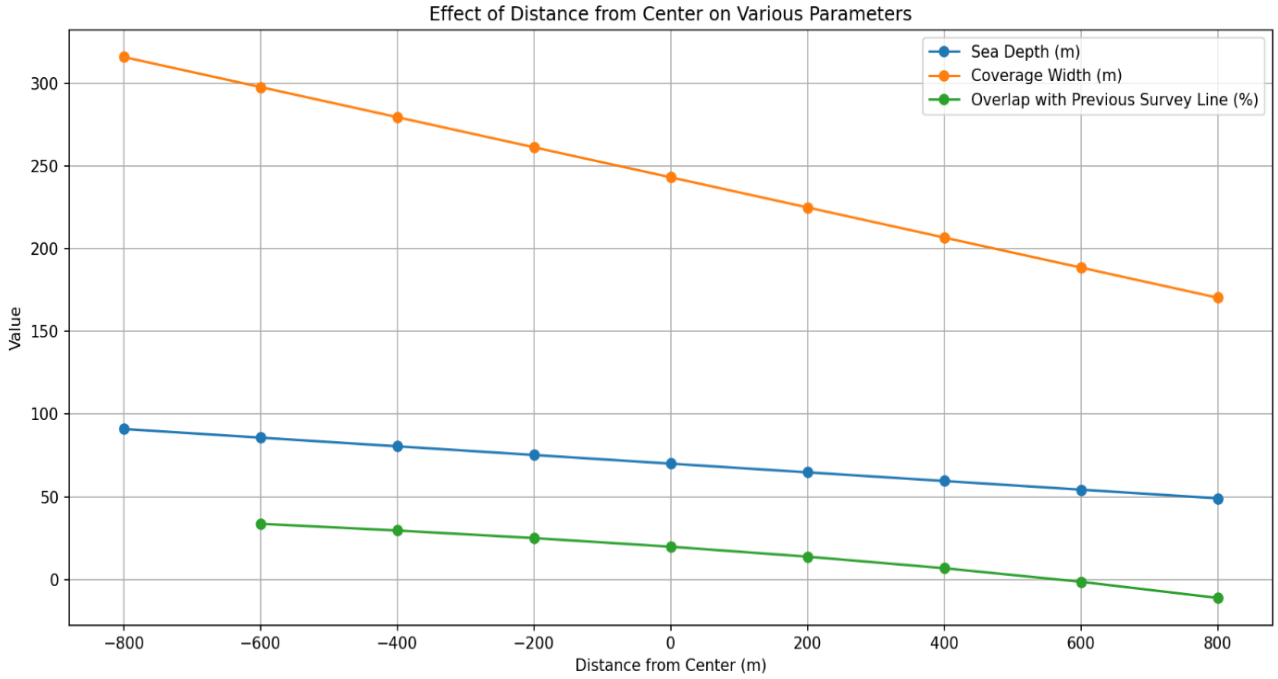

Figure 3. Impact of distance from the center point on various parameters

3.1.3 Sensitivity Analysis of Simulated Seabed Topography

(1) Sensitivity Analysis for Beam Angle

In the sensitivity analysis, the beam angle of the multibeam transducer is reduced to 80^0, with a slope of 1.5 °, and the water depth at the central point of the sea area is 70 m[8].

The results indicate that when the beam angle decreases, both the coverage width and overlap rate significantly reduce, leading to the conclusion: the beam angle has a considerable impact on coverage width and overlap rate. Selecting too small a beam angle results in a smaller measurement range and lower measurement efficiency.

Table 2. Sensitivity Analysis of Opening Angle Size

Distance from the center point/m	Water depth/m	Coverage width/m	Overlap rate with the previous survey line/%
-800	90.949	152.76	——
-600	85.712	143.96	-33.91
-400	80.474	135.16	-42.10
-200	75.237	126.37	-51.35
0	70	117.57	-61.88
200	64.763	108.77	-74.00
400	59.526	99.98	-88.06
600	54.288	91.18	-104.61
800	49.051	82.39	-124.35

Similarly, it is easy to understand that when the opening angle increases, both the coverage width and overlap rate will increase. However, considering the impact of detection density on accuracy and energy consumption issues, we should also avoid choosing a transducer with too large an opening angle.

(2) Sensitivity Analysis of Seabed Slope

In the sensitivity analysis, the opening angle of the multibeam transducer is set to 120°, the slope increases to 4°, and the water depth at the center of the sea area is 70 m.

The results are as follows: as the slope increases, the water depth, coverage width, and overlap rate all change significantly. Therefore, we conclude that the slope has a significant impact on water depth, coverage width, and overlap rate. When the slope is large, it is more effective in deep-sea areas to choose a smaller opening angle and increase the spacing between survey lines, while in shallow-sea areas, it is better to choose a larger opening angle and decrease the spacing.

Table 3. Sensitivity Analysis of Seabed Slope

Distance from the center point/m	Water depth/m	Coverage width/m	Overlap rate with the previous survey line/%
-800	125.96	443.85	——
-600	111.96	394.56	48.60
-400	97.97	345.27	42.18
-200	83.99	295.99	33.93
0	70	246.70	22.93
200	56.01	197.41	7.53
400	42.03	148.12	-15.55
600	28.04	98.83	-54.00
800	14.06	49.55	-130.81

(3) Sensitivity Analysis of Seabed Depth

In the sensitivity analysis, the opening angle of the multibeam transducer is set to $120°$, the slope is $1.5°$, and the water depth at the center of the sea area increases to $100m$.

The results are as follows: as the water depth increases, both the coverage width and overlap rate increase to a certain extent. We conclude that the water depth has a certain impact on the coverage width and overlap rate. In deeper sea areas, we should appropriately increase the spacing between survey lines and choose a suitable transducer opening angle.

Table 4. Sensitivity Analysis of Seabed Depth

Distance from the center point/m	Water depth/m	Coverage width/m	Overlap rate with the previous survey line/%
-800	120.95	419.99	——
-600	115.712	401.80	50.10
-400	110.474	383.61	47.84
-200	105.237	365.43	45.37
0	100	347.24	42.65
200	94.763	329.06	39.65
400	89.526	310.87	36.31
600	84.288	292.69	32.59
800	79.051	274.50	28.40

3.2. Results and Analysis under the General Case of Non-parallelism between Survey Lines and Isobaths

3.2.1 Establishment and Solution of the Model in the Special Case of Parallelism between Survey Lines and Isobaths

In this scenario, the direction of the ship's survey line is generally extended relative to Question One. It is known that the angle between the direction of the survey line and the normal of the seabed slope projected on the horizontal plane is \beta, with the special case of parallelism between the survey line and the isobaths being the situation where $\beta = \frac{\pi}{2}$ [9].

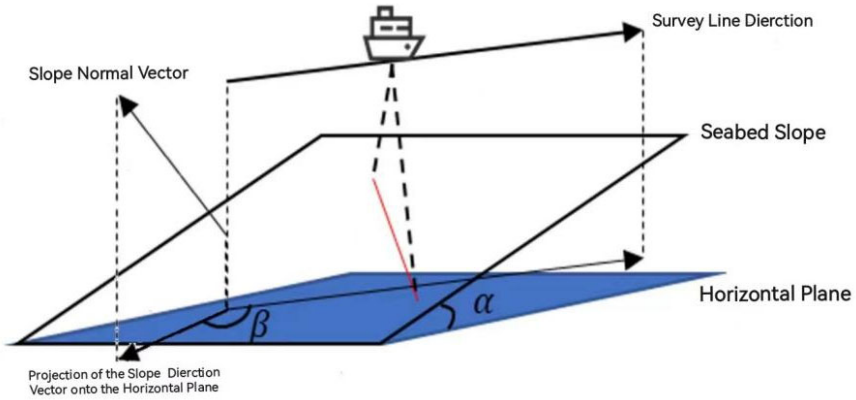

Figure 4. Actual Background of the General Case of Non-parallelism between Survey Lines and Isobaths

As shown in Figure 4, In this scenario, our study can still establish a planar geometric model to describe the coverage width under different conditions. Considering that the cross-section of the slope in different directions is still an inclined surface, just with different tilt angles, we only need to determine the slope angles corresponding to different survey line directions, which can then be transformed into a model for the special case where survey lines are parallel to isobaths for solving.

This study divides the problem's transformation and solution into the following three steps:

Step One: Calculate the depth of the seabed at the location of the survey ship

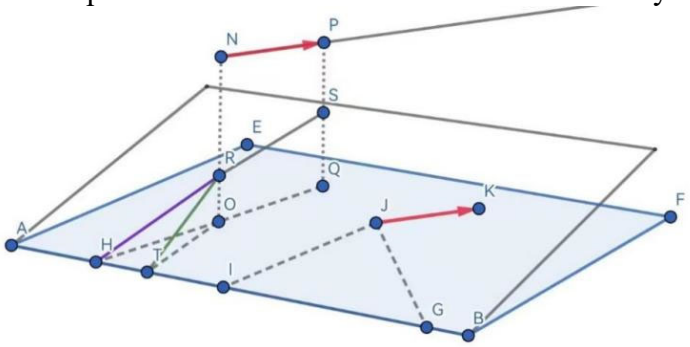

Figure 5. Calculate the depth of the seabed where the survey ship is located

As shown in Figure 5, let point N be the center of the sea area, and point P be the location of the survey ship. The direction of $\overrightarrow{NP}$ is the survey line direction. In the special case where the survey line is parallel to the contour line, we set D as the seabed depth at the center of the sea area, and X as the distance from the survey ship to the center of the sea area [10]. Here, $D = |NR|, X = |NP|$. We now need to calculate the depth PS of the survey ship. First, we list some known geometric relationships:

$$OT \perp AB, RO \perp ABFE \tag{19}$$

$$\angle TOQ = \angle IJK = \beta \tag{20}$$

$$\angle RTO = \alpha \tag{21}$$

$$\Rightarrow \begin{cases} \angle HOT = \pi - \beta \\ \angle HTO = \dfrac{\pi}{2} \end{cases} \tag{22}$$

Let α_0 be the angle formed by the survey line direction intersecting with the seabed slope and horizontal plane:

$$\angle SHQ = \angle RHO = \alpha_0 \tag{23}$$

Given $\angle RTO = \alpha$, in $rt \triangle ROT$ and $rt \triangle ROH$, we have:

$$\begin{cases} tan(\alpha_0) = \dfrac{|RO|}{|HO|} \\ tan(\alpha) = \dfrac{|RO|}{|TO|} \end{cases} \tag{24}$$

$$\Rightarrow \frac{tan(\alpha_0)}{tan(\alpha)} = \frac{|TO|}{|HO|} = sin(\beta) \tag{25}$$

$$\Rightarrow |PS| = |NR| - |NP|tan(\alpha_0) = |NR| - |NP|tan(\alpha)sin(\beta) \tag{26}$$

$$\Rightarrow |PS| = D - Xtan(\alpha)sin(\beta) \tag{27}$$

The above equation can determine the water depth at a specific point under certain conditions.

Step 2: Calculate the angle of intersection between the plane perpendicular to the survey line direction and the seabed slope and horizontal plane

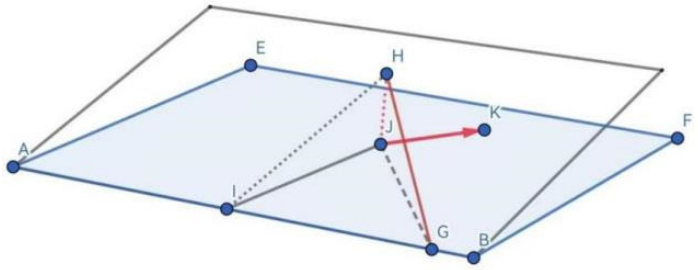

Figure 6. Calculating the angle of intersection between the plane perpendicular to the survey line direction and the seabed slope and horizontal plane.

As shown in Figure 6, point H corresponds to point S in the previous figure, and point J corresponds to point Q; the other points correspond accordingly. The direction of $\overrightarrow{JK}$ is the side line direction. Plane HJI is perpendicular to the survey line direction. We now need to calculate the angle $\angle HGJ$. Let $\angle HGJ = \alpha_1$. This allows us to transform the model in plane HGJ into the special case where the survey line is parallel to the contour line. First, we organize the following geometric relationships:

$$JI \perp AB, HJ \perp ABFE \tag{28}$$

$$\begin{cases} \angle IJK = \beta \\ \angle HIJ = \alpha \\ \angle GJK = \dfrac{\pi}{2} \end{cases} \tag{29}$$

$$\Rightarrow \angle IJG = \angle IJK - \angle GJK = \beta - \frac{\pi}{2} \tag{30}$$

In right triangles $rt \triangle HJI$ and $rt \triangle HJG$, we have:

$$\begin{cases} tan(\alpha) = \dfrac{|HJ|}{|IJ|} \\ tan(\alpha_1) = \dfrac{|HJ|}{|GJ|} \end{cases} \tag{31}$$

$$\Rightarrow \frac{tan(\alpha_1)}{tan(\alpha)} = \frac{|IJ|}{|GJ|} = sin(\pi - \beta) \tag{32}$$

After simplifying:

$$tan(\alpha_1) = tan(\alpha)sin(\pi - \beta) = tan(\alpha)sin(\beta) \tag{33}$$

$$\Rightarrow \alpha_1 = arctan\big(\, tan(\alpha)sin(\beta)\big) \tag{34}$$

Step 3: Calculate the coverage width W

Through the above discussion, we have successfully transformed the problem in general situations into a model that has been successfully solved in special cases, as shown in Figure 7:

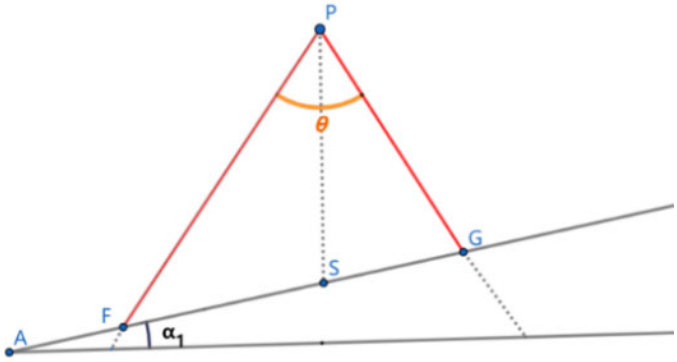

Figure 7. Calculating the coverage width W

From the conclusion of Step 1, we know:

$$|PS| = |NR| - |NP|tan(\alpha_0) = D - Xtan(\alpha)sin(\beta) \tag{35}$$

In this study, the coverage width is set to $L = FG$. From the established model, we obtain:

$$W = \frac{|PS|sin\left(\frac{\theta}{2}\right)}{cos\left(\alpha_1 - \frac{\theta}{2}\right)} + \frac{|PS|sin\left(\frac{\theta}{2}\right)}{cos\left(\alpha_1 + \frac{\theta}{2}\right)} \tag{36}$$

$$\Rightarrow W = \frac{[D - Xtan(\alpha)sin(\beta)]sin\left(\frac{\theta}{2}\right)}{cos\left(arctan\big(tan(\alpha)sin(\beta)\big) - \frac{\theta}{2}\right)} + \frac{[D - Xtan(\alpha)sin(\beta)]sin\left(\frac{\theta}{2}\right)}{cos\left(arctan\big(tan(\alpha)sin(\beta)\big) + \frac{\theta}{2}\right)} \tag{37}$$

3.2.2 Simulation results of the seabed topography

For intuitive presentation, this study established a simulation of the seafloor topography and performed actual calculations. The seafloor topography set the opening angle of the multi-beam transducer to 120°, with a slope of 1.5°, and a specific scenario where the water depth at the center of the sea area is 120m. The results for this scenario are calculated as follows: Given the simulated sea area has a flat slope, deeper in the west and shallower in the east, the analysis of the results is as follows(Table 5):

(1) When ensuring the measurement line direction remains unchanged, as the ship's position varies arithmetically from the center point, the coverage width forms an arithmetic sequence, and the difference increases as the angle between the measurement line and the plane becomes larger.

(2) When ensuring the ship's distance from the center remains constant, the coverage width shows symmetry with the measurement line angle: maximum at 0° and minimum at 180°.

(3) As the ship's distance from the center increases, the variation range of the coverage width under different measurement line angles also increases.

(4) As the direction of the measurement line changes, the variance in coverage width at different center distances shows symmetry.

Table 5. Simulation Results of the Seabed Topography

Coverage width/m		Distance from the survey ship to the center of the sea area/nautical miles							
		0	0.3	0.6	0.9	1.2	1.5	1.8	2.1
Angle of the survey line direction/°	0	415.692	466.091	516.49	566.889	617.288	667.686	718.085	768.484
	45	416.192	451.872	487.52	523.232	558.912	594.592	630.273	665.953
	90	416.692	416.692	416.692	416.692	416.692	416.692	416.692	416.692
	135	416.192	380.511	344.831	309.151	273.471	237.791	202.11	166.43
	180	415.692	365.293	314.894	264.496	214.097	163.698	113.299	62.9002
	225	416.192	380.511	344.831	309.151	273.471	237.791	202.11	166.43
	270	416.692	416.692	416.692	416.692	416.692	416.692	416.692	416.692
	315	416.192	451.872	487.52	523.232	558.912	594.592	630.273	665.953

4. Conclusions

The operational principle of the multibeam seabed depth measurement system involves conducting acoustic measurements underwater to determine the depth of the seabed and related topographical features. The system emits multiple acoustic beams simultaneously, typically in a vertical plane to the navigation path, and then uses receiving sensors to capture the acoustic waves reflected back from the seabed. The goal of this research is to calculate information such as the seabed depth, the coverage width of the survey lines, and the overlap rate between survey lines, especially in uneven seabed conditions, by analyzing these received acoustic wave data.

Firstly, this study discussed the special case of survey lines being parallel to isobaths. It defined concepts such as coverage width and overlap rate, and then employed the Law of Sines and triangle-solving methods to calculate physical parameters such as the seabed depth, coverage width, and overlap rate with the previous survey line, considering especially the sensitivity of these parameters to the seabed slope, depth, and the emission angle of the acoustic beams.

Following that, the research delved into the general case of survey lines not being parallel to isobaths. By solving for the intersection points of the seabed cross-section measured by the vessel with the seabed slope, and the angles between these intersections and the horizontal plane, the problem was remodeled and calculated. This allowed us to continue using the model developed under the parallel circumstance to calculate the survey line's coverage width. Similarly, we examined the influence of depth, slope, and the opening angle of the acoustic beams on these parameters.

Through the application of computational geometric principles to study the performance of the multibeam seabed depth measurement system in uneven seabed conditions, this research provides an effective method usable in sea areas with complex seabed topography. This contributes to expanding the application scope of the multibeam seabed depth measurement system, particularly in the field of uneven seabed depth measurement, offering more simplified computational methods for related domains.

References

[1] QIN Chaojie YAO Rui. Application of multi-beam technology in underwater topographic survey of Huaihe River Basin[J].Water Resources Informatization,2023(02):61-64.DOI:10.19364/j.1674-9405.2023.02.012.

[2] CHENG Fang,HU Youcheng. Research on the Optimization Method For Survey Line Layout In Multi Beam Survey[J].Ocean Technology,2016,35(02):8791.

[3] Wang J ,Tang Y ,Jin S , et al. A Method for Multi-Beam Bathymetric Surveys in Unfamiliar Waters Based on the AUV Constant-Depth Mode[J]. Journal of Marine Science and Engineering,2023,11(7).

[4] Aniol M ,Jordi P ,David A , et al. Compression of Multibeam Echosounders Bathymetry and Water Column Data[J]. Remote Sensing,2022,14(9).

[5] Qiang G , Chuanyu F ,Yikang C , et al. Application of multi-beam bathymetry system in shallow water area[J]. Journal of Physics: Conference Series,2023,2428(1).

[6] WANG Junsen ,JIN Shaohua, BIAN Zhigang, et al. Residual Correction of the Rolling Motion in Multibeam Bathymetry Using Overlapping Area of Adjacent Survey Lines[J].Ocean Technology,2023,42(04):35-42.

[7] LIU Lin.Reasons and Solutions for the Distortion of Multibeam Sounding Data[J].Value Engineering,2023,42(21):125-128.

[8] DONG Yu. Research on the Application of Multibeam Bathymetry System in Marine Hydrographic Survey[J].Engineering Technology Research,2023,8(15):122-124.DOI:10.19537/j.cnki.2096-2789.2023.15.040.

[9] MA Zhenghai LIN Dang LI Shengxuan, et al. Underwater terrain mapping of Jingjiangmen river reach based on multi-beam bathymetry system[J].Express Water Resources & Hydropower Information,2022,43(12):36-40.DOI:10.15974/j.cnki.slsdkb.2022.12.006.

[10] Grządziel A . Method of Time Estimation for the Bathymetric Surveys Conducted with a Multi-Beam Echosounder System[J]. Applied Sciences,2023,13(18).